SUPPLEMENTARY MATERIAL1

Integrating olivine diffusion chronometry with monitoring data to decipher the magma dynamics at the Fani Maoré volcano

Karoline Brückel[1], Etienne Médard[1], Fidel Costa[2], Carole Berthod[2,3], Pauline Verdurme[1,4], Patrick Bachèlery[1], Lise Retailleau[2], Jean-Christophe Komorowski[2], Lucia Gurioli[1]

[1] Université Clermont Auvergne, CNRS, IRD, OPGC, Laboratoire Magmas et Volcans, F-63000 Clermont-Ferrand, France

[2] Institut de physique du globe de Paris, Université Paris Cité, CNRS, F-75005 Paris, France

[3] Observatoire volcanologique et sismologique de la Guadeloupe, Institut de physique du globe de Paris, 97113, Gourbeyre, France

[4] GEOMAR Helmholtz Centre for Ocean Research Kiel, Kiel, Germany

Corresponding author: Karoline Brückel (karoline.bruckel@uca.fr)

This Supplementary Material1 contains additional figures referred to in the man text. The following figures are shown:

Fig. S1: Summary of the petrologic and geochemical evolution of the Fani Maoré eruption

Fig. S2: Comparison of a single step and a two-step (including growth) diffusion model.

Fig. S3: Percent of embayments in olivine of Phase 2 and Phase 3a.

Fig. S4: BSE images of FM mineral textures supplementary to Fig. 2 in the main text.

Fig. S5: Comparison of the textures and Mg content of olivine, clinopyroxene, and orthopyroxene antecrysts in FM.

Fig. S6: Minor element concentration (Ca, Mn, Ni, P) of olivine in Phase 2, 3a.

Fig. S7: Trace element concentrations in olivine and minor elements in magnetite of FM shown for all eruptive phase 1 to 3b.

Fig. S8: Histograms of diffusion timescales for the different FM Timespans using Fo, Mn, and Ni profiles.

Fig. S9: Comparison between timescales derived from rims and embayments of the same olivine.

Fig. S10: Textures in Phase 2 and 3a that could imply a change in Fe^{3+}/Fe^{2+} ratio and redox state.

Fig. S11: X-ray maps of the P distribution in selected olivine from Phase 2 and Phase 3a.

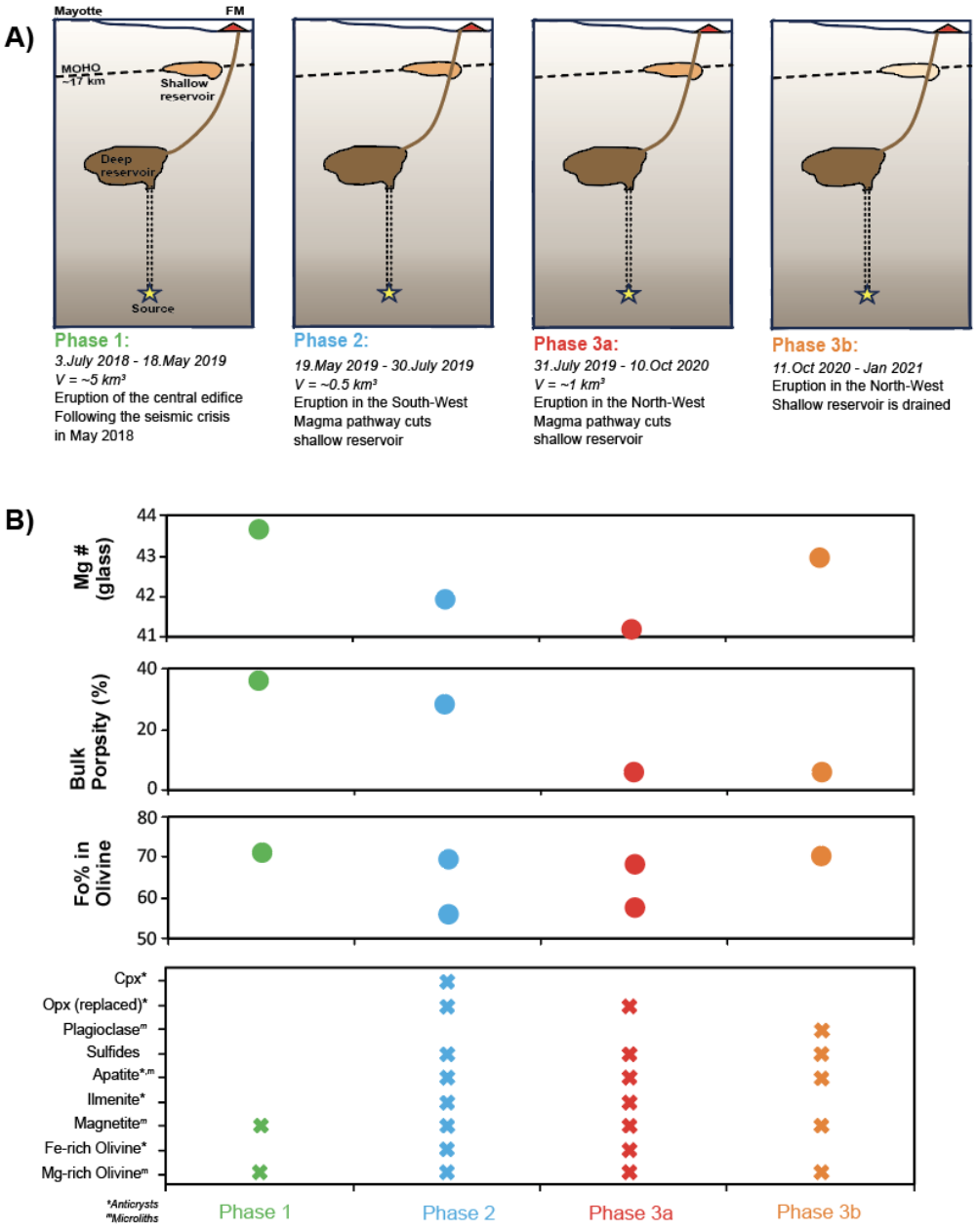

Fig. S1: Summary of petrologic and geochemical evolution of the Fani Maoré eruption according to Berthod et al. (2021, 2022) and Verdurme et al. (2024). (**A**) Timing, eruption volume and location for the three different FM phases, as well as the suggested evolution history. (**B**) Evolution of Mg# in FM glass, Bulk Porosity, Fo of Olivine and Mineral Assemblage for the three phases.

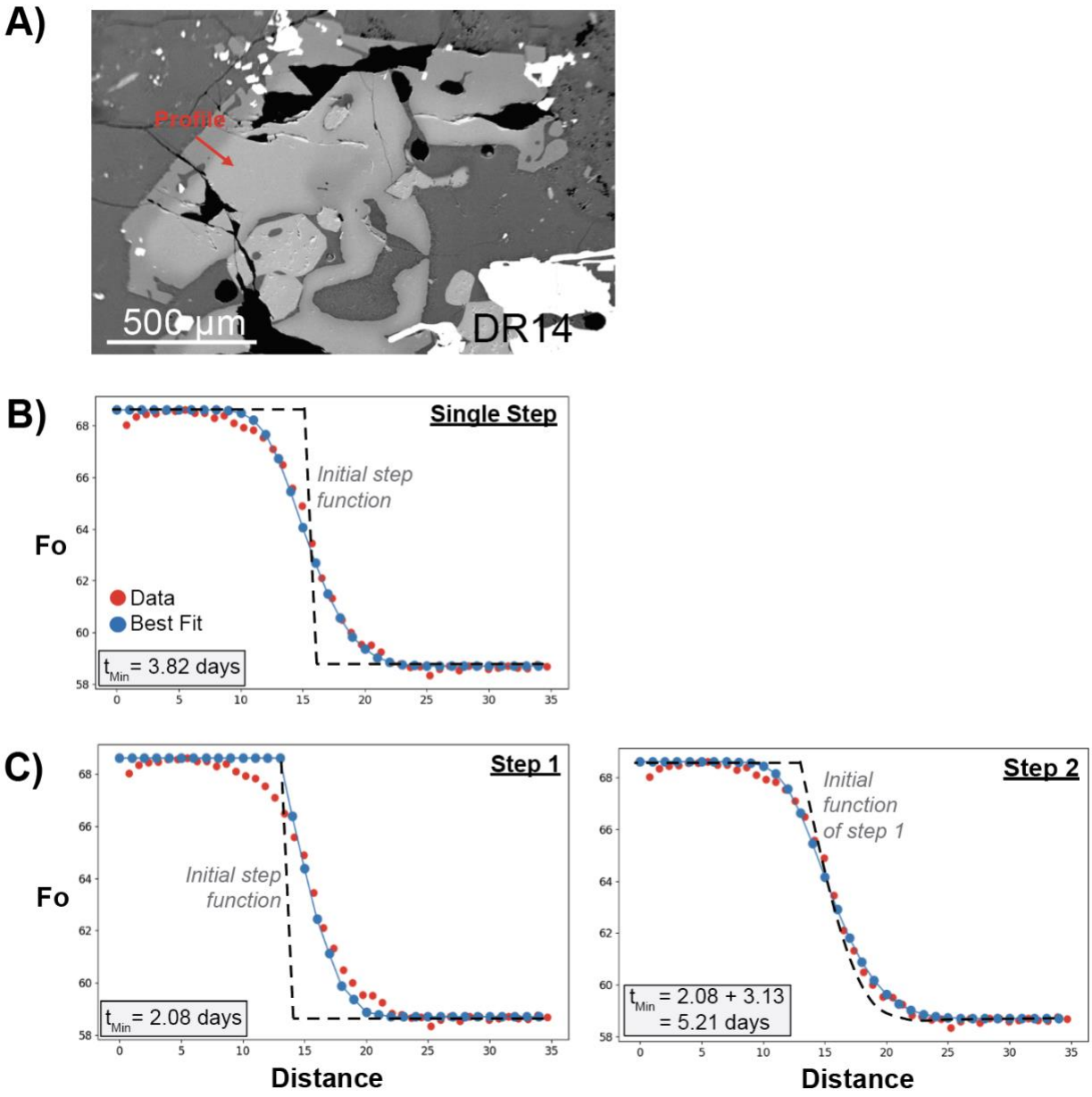

Fig. S2: Comparison of a single step and a two-step model (assuming rim growth during diffusion) for diffusion. (**A**) BSE image of Phase 3a zoned olivine with the diffusion profile shown as red arrow. (**B**) Single Step diffusion model not distinguishing diffusion and growth. (**C**) Two Step model, where diffusion occurs before and after growth. For Step 2 the best fit function of Step 1 is used as the initial function. Not that the two models result in similar timescales.

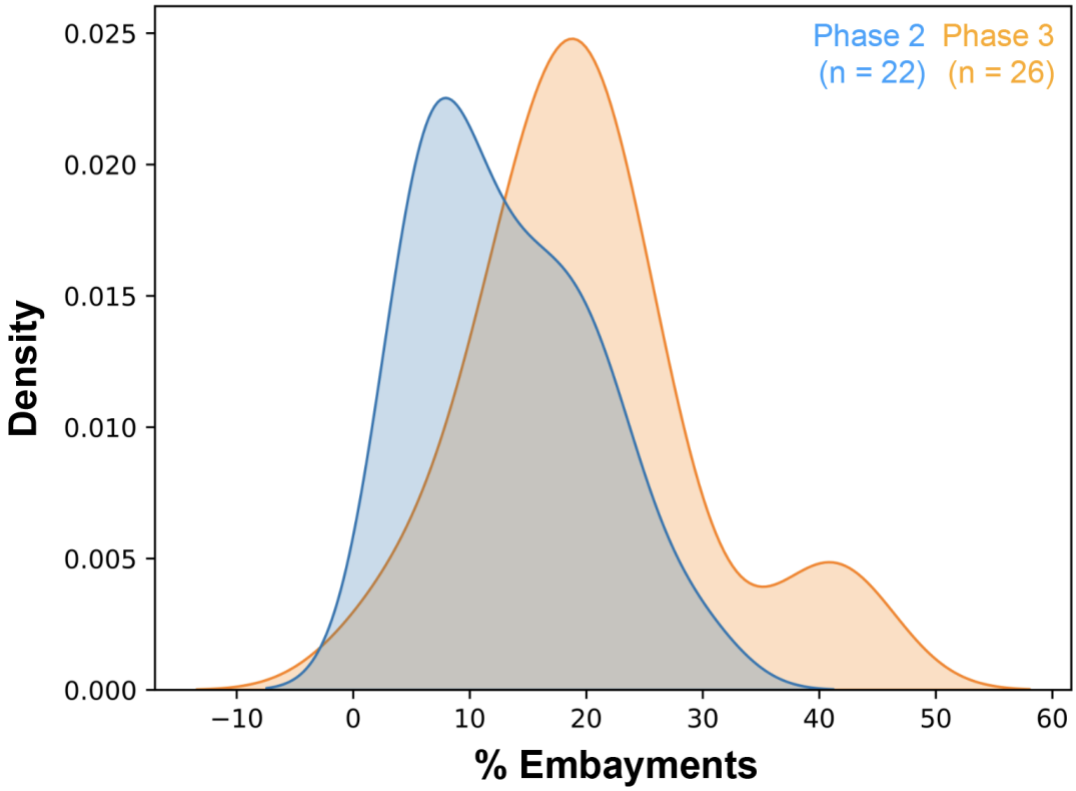

Fig. S3: Percent of the area of the crystal that has filled with embayments for olivine of Phase 2 (blue) and of Phase 3a (orange).

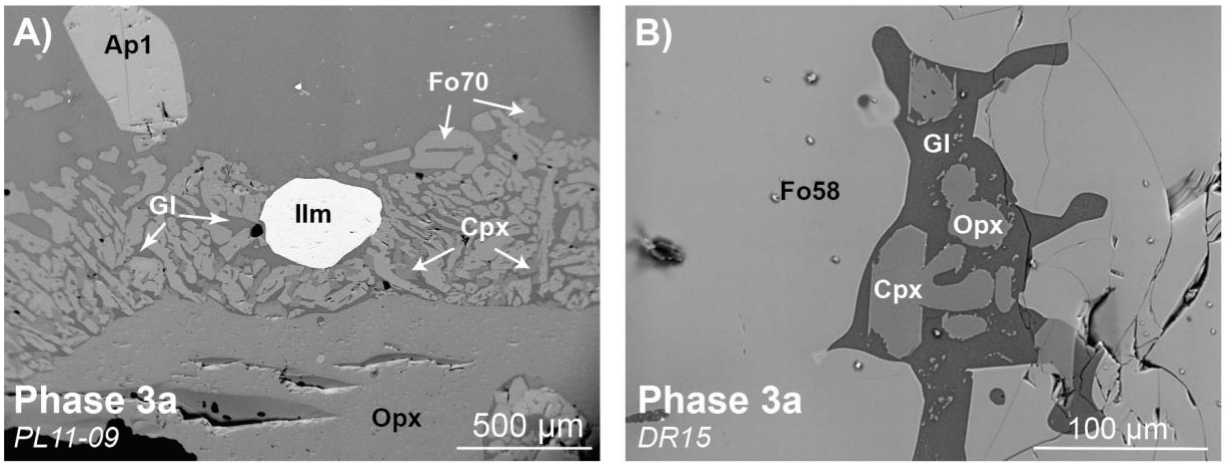

Fig. S4: BSE images of FM mineral textures supplementary to Fig. 2. (**A**) Orthopyroxene with spongy breakdown rim of olivine (Fo70), clinopyroxene and glass in the vicinity of ilmenite and apatite associated with the shallower reservoir. (**B**) Trachytic melt inclusion in olivine antecryst core with irregular shape and small pyroxenes.

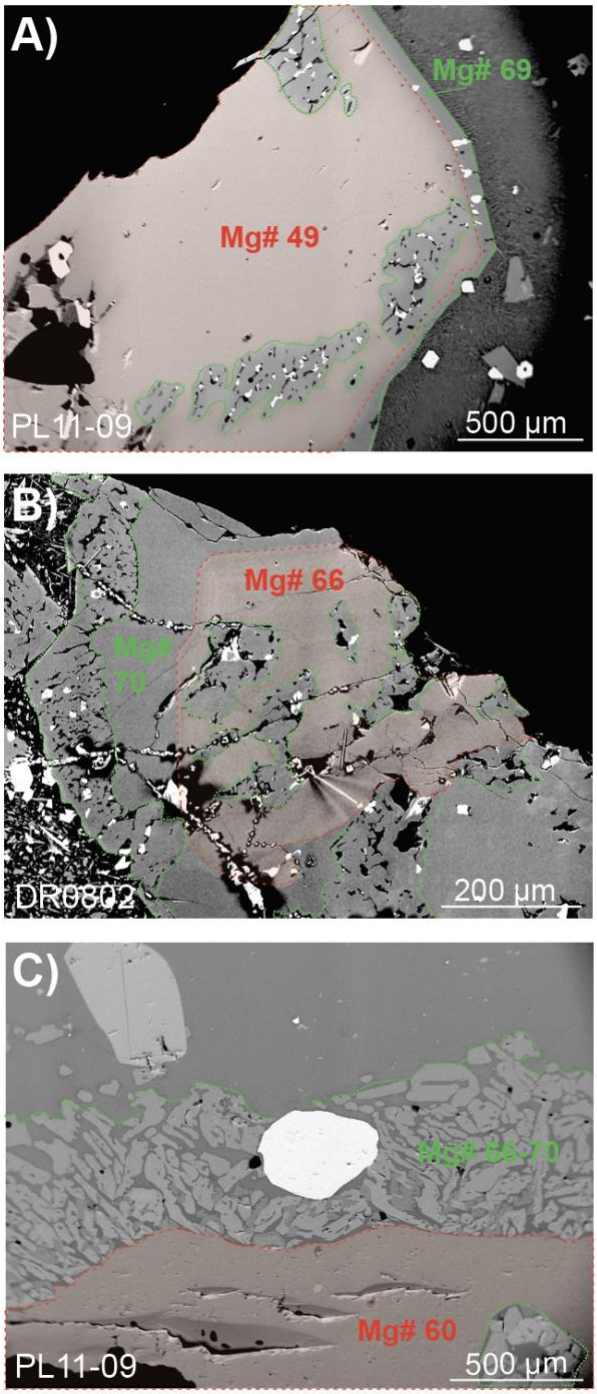

Fig. S5: Antecrysts found in FM. Fe-rich cores are outlined and shaded in red; Mg-rich areas are outlined in green. (**A**) Olivine in phase 3a with Fe-rich core and Mg-rich rim. The core has areas with magnetite-rich embayments surrounded by Mg-rich olivine. (**B**) Clinopyroxene in Phase 2 found by Berthod et al. (2021). Fe-rich core is surrounded by Mg-rich rim that has an outer part with a spongy/embayed texture occasionally filled with magnetite. Core has patches of Mg-rich, porous/spongy clinopyroxene. (**C**) Fe-rich orthopyroxene surrounded by a spongy rim of Mg-rich olivine and clinopyroxene.

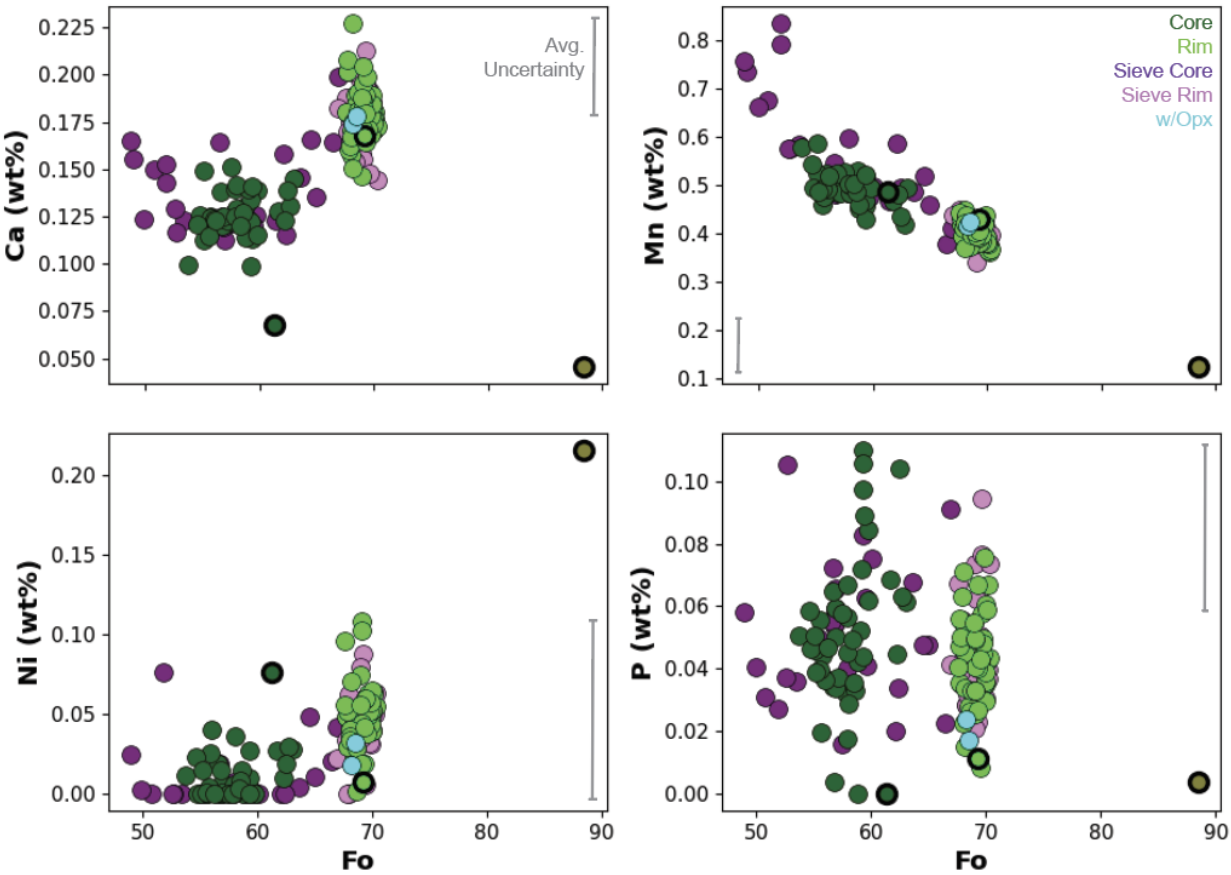

Fig. S6: Minor element concentration (Ca, Mn, Ni, P) of olivine in Phase 2, 3a divided by the texture (simple zoned olivine core and rim; sieve olivine core and rim; and olivine in the orthopyroxene breakdown rim) Triple-zoned olivine is marked with a thick black edge.

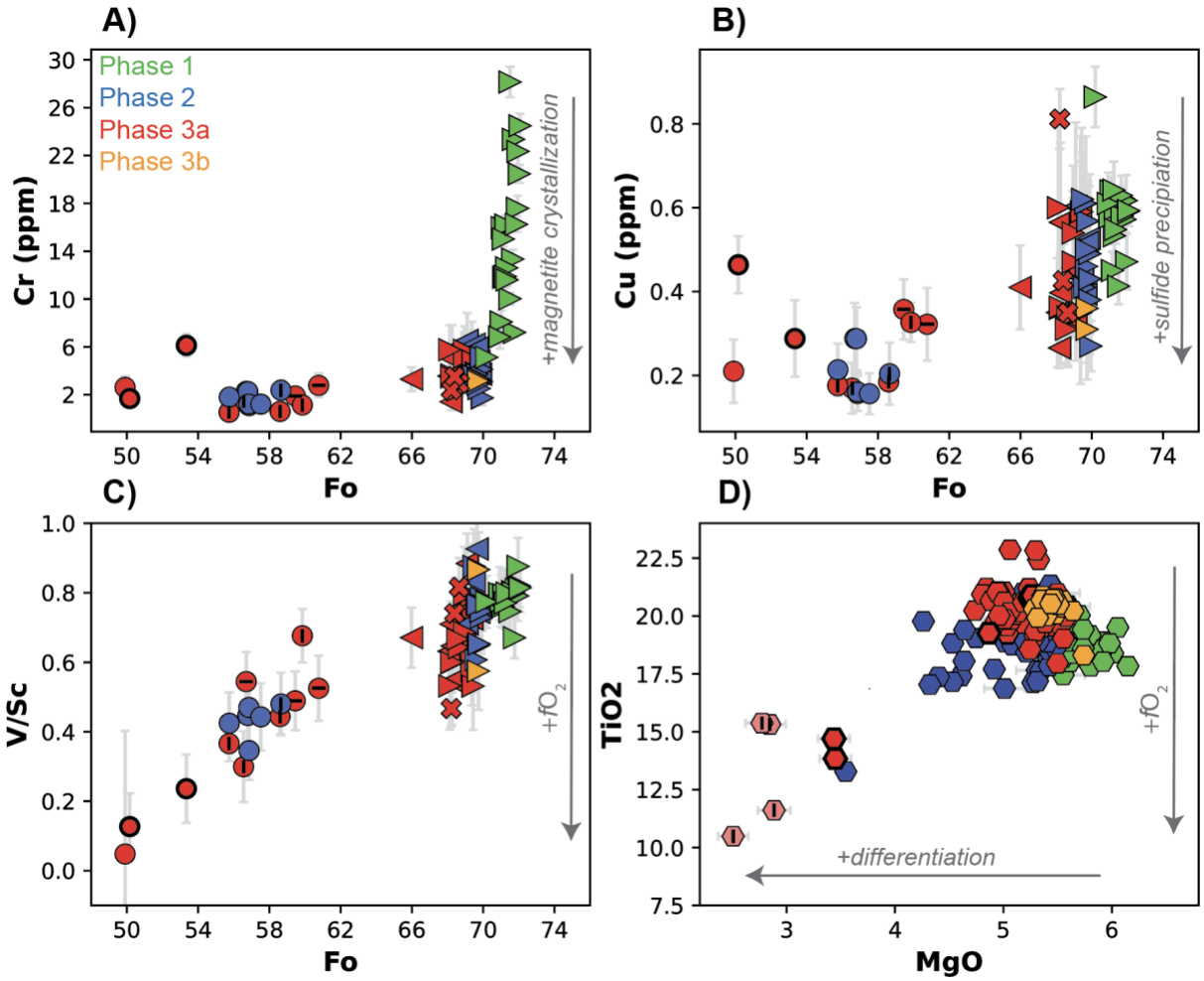

Fig. S7: Trace element concentrations in olivine (**A-C**) and minor elements in magnetite (**D**) of Phase 1 to 3b. Symbols: (**A-C**) olivine core (circle), olivine rim (triangle left), olivine microlites/micro-phenocrysts (triangle right), olivine in orthopyroxene rim (cross), sieve olivine (thick edge), olivine with trachytic melt inclusion (horizontal bar), olivine with tephri-phonolitic melt inclusion (vertical bar), and (**D**) magnetite in tephri-phonolitic melt inclusions (pink, vertical bar). **A)** Lower Cr in olivine rims and microlites of phase 2, 3 compared to Phase 1 implies crystallization of spinel (magnetite). **B)** Lower Cu in olivine rims and microlites of Phase 2, 3 compared to Phase 1 implies precipitation of sulfides. **C)** Lower V/Sc in olivine cores of Phase 2, 3a, suggests a more oxidized environment than for Phase 1, 3b and olivine rims/microlites of Phase 2, 3a. **D)** Lower TiO_2 and MgO in magnetite of Phase 2 compared to Phase 1, 3 suggests a more oxidized and differentiated environment, similarly, to that of magnetite in melt inclusions of Phase 3a.

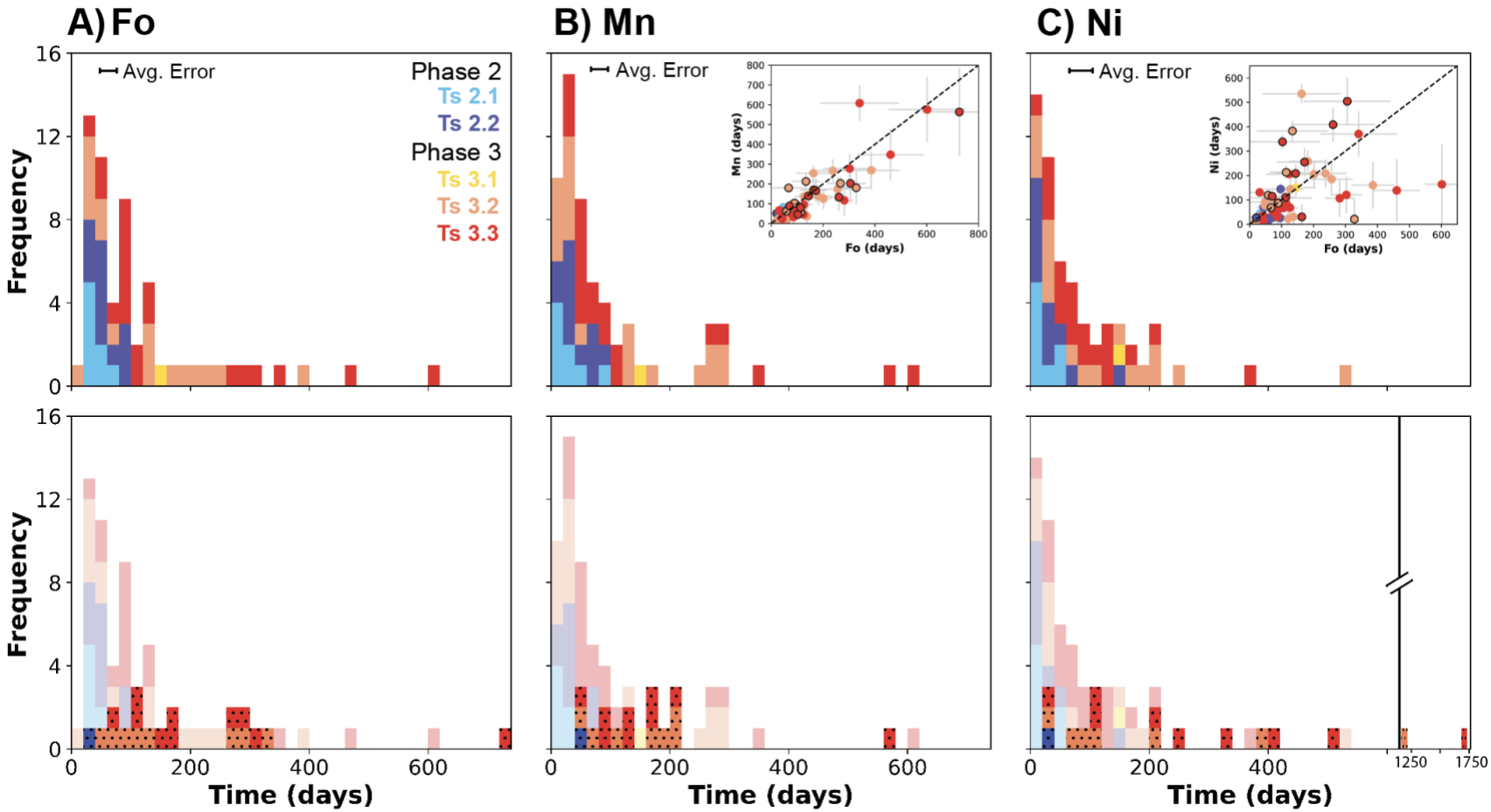

Fig. S8: Histograms of diffusion timescales using **A)** Fo, **B)** Mn and **C)** Ni profiles in olivine of the five different Timespans. Top row shows rim profiles, bottom row shows profiles along embayments. Inlets in **B)** show a good correlation (nearly 1:1) of the timescales using Fo profiles and those of the Mn profiles. The correlation for Ni as inlet in **C)** is not as good, particularly for embayment profiles (circles outlined in black).

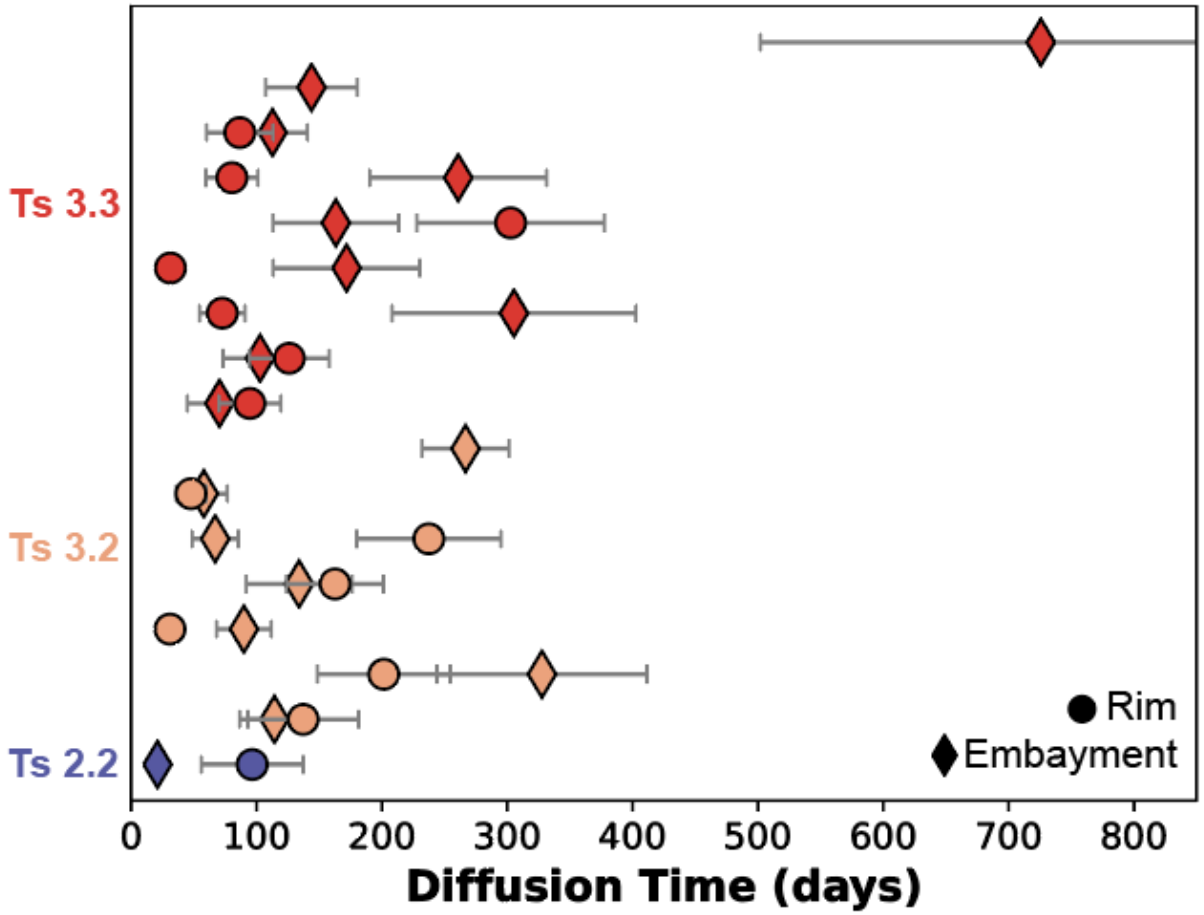

Fig. S9: Fo diffusion times from profiles taken along olivine rims (circles) compared to those taken along embayments (diamonds) in Timespans 2.2, 3.2, 3.3.

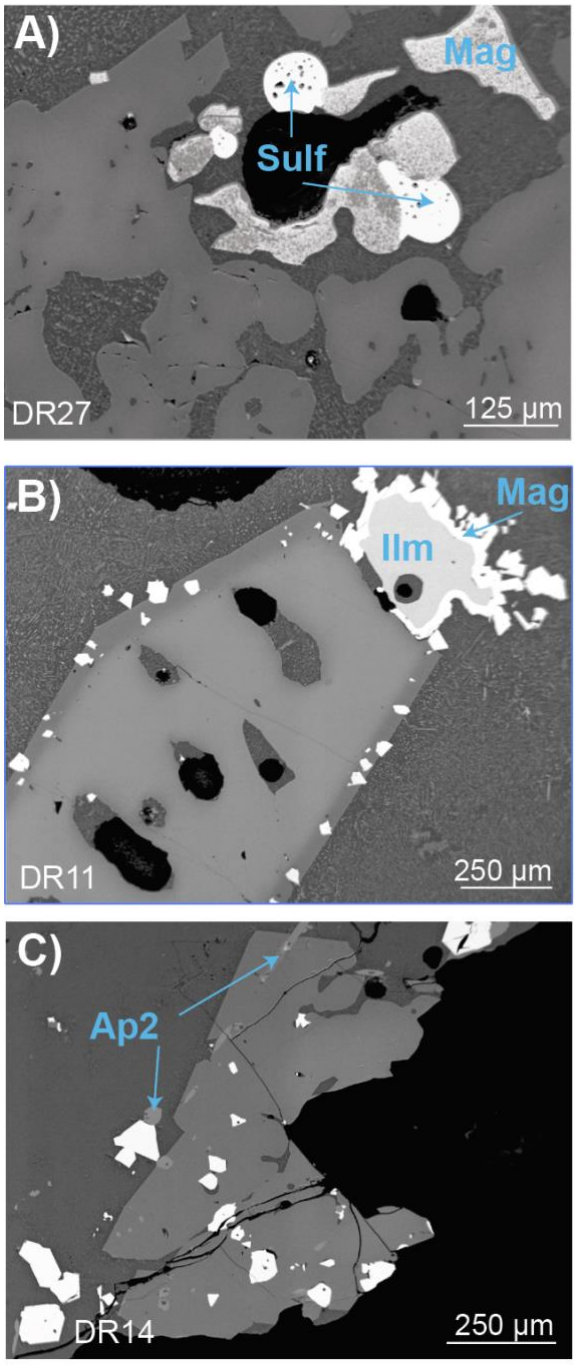

Fig. S10: Textures in Phase 2 and 3a that imply a change in Fe^{3+}/Fe^{2+} ratio and redox state. (**A**) Sulfide droplets in embayments of olivine cores. (**B**) Magnetite rim around ilmenite associated with the olivine core and magnetite intergrown with the Mg-rich olivine rim. (**C**) Small, euhedral apatite intergrown with the Mg-rich olivine rims.

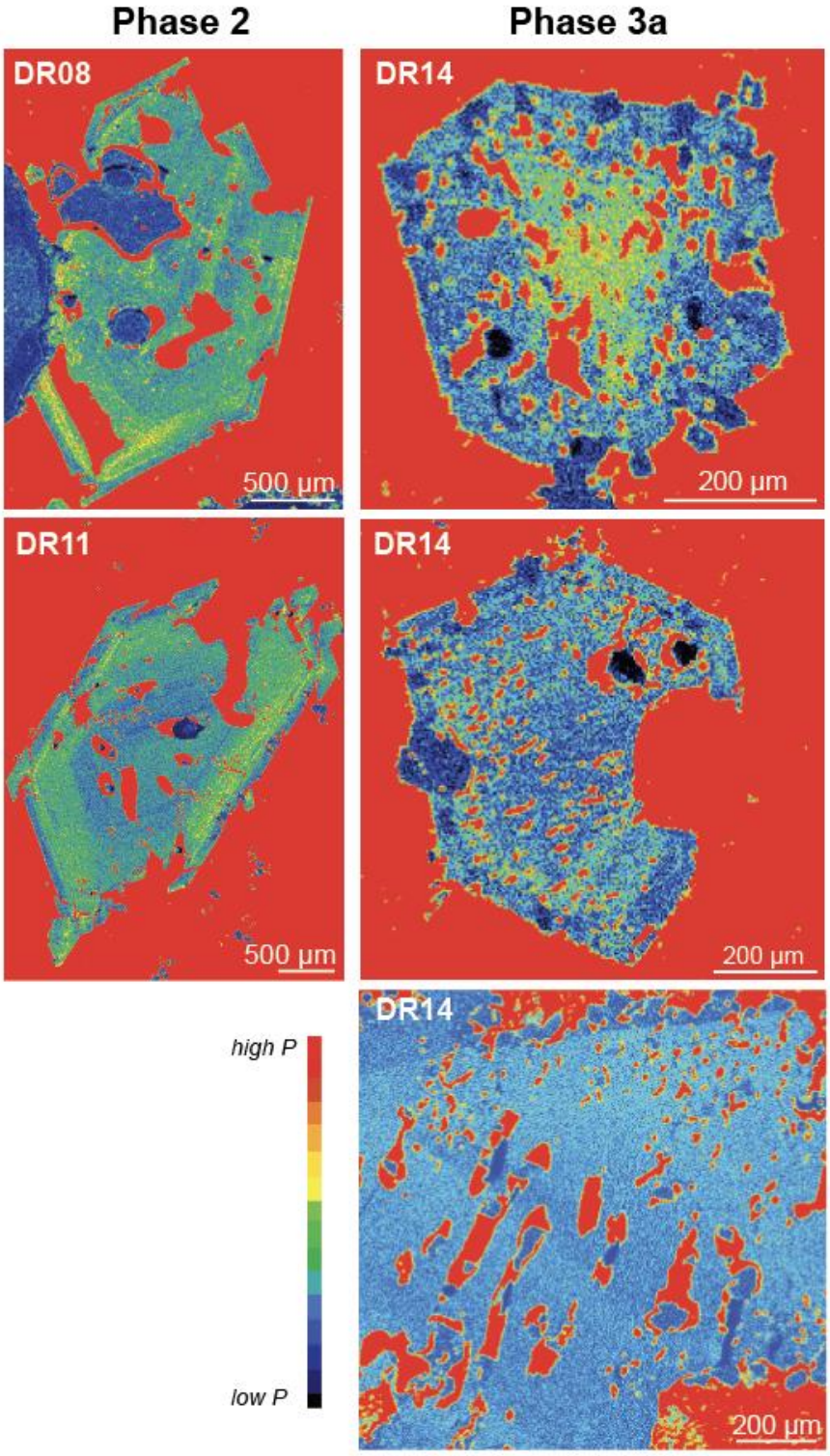

Fig. S11: X-ray maps of P distribution in olivine antecrysts of Phase 2 and Phase 3a. Note P zoning is cut by embayments implying these are dissolution textures. Phase 2 olivines with fewer embayments have more P zoning, whereas Phase 3a olivines that have a more intensive sieve texture do not show consistent zoning in P maps.